Predictive Markers of LRRK2 Inhibition in Biofluids

Shijie Wang[1++], Kaela Kelly[1++], Nathalie Schussler[2], Sylviane Boularand[2], Laurent Dubois[2], Frank Hsieh[3], Elizabeth Tengstrand[3], Jonathan M. Brotchie[4], James B. Koprich[4], Andrew B. West[1*]

[1] Duke Center for Neurodegeneration Research, Department of Pharmacology and Cancer Biology, Duke University, Durham, North Carolina, USA

[2] Rare & Neurologic Diseases Research, Sanofi, Chilly Mazarin, France

[3] Nextcea, Inc., Woburn, MA, USA

[4]Atuka Inc., Toronto, Ontario, Canada

[++] Equal contribution.

*C.A. Information: andrew.west@duke.edu, 3 Genome Court, Durham, North Carolina, 27710 USA

Abstract

Hyper-activated LRRK2 is linked to Parkinson's disease susceptibility and progression. Quantitative measures of LRRK2 inhibition, especially in the brain, may be critical in the clinical development of successful LRRK2-targeting therapeutics. In this study, three structurally distinct, brain-penetrant, and selective LRRK2 small-molecule kinase inhibitors (PFE-360, MLi2, and RA283) were orally administered to groups of cynomolgus macaques at different doses. Biofluid markers with proposed predictive value for assessing LRRK2 inhibition were measured from samples of blood, urine, and cerebral-spinal fluid (CSF). LRRK2 kinase inhibition led to consistent reduced pS935-LRRK2 and pRab10 proteins in blood mononuclear cells, reduced exosome LRRK2 protein and di-docosahexaenoyl (22:6) bis (monoacylglycerol) phosphate in urine, and reduced exosome LRRK2 and autophosphorylated pS1292-LRRK2 protein in CSF. Incomplete LRRK2 kinase inhibition reduced LRRK2 protein secretion in exosomes whereas high drug exposures may reduce both exosome and tissue levels of LRRK2 protein. These orthogonal pairs of markers for LRRK2 inhibition in urine and CSF can be used in combination with blood markers to non-invasively monitor the potency of LRRK2-targeting therapeutics in the brain and periphery.

Introduction

Leucine-rich repeat kinase 2 (LRRK2) small molecule kinase inhibitors and anti-sense oligonucleotides have demonstrated neuroprotective efficacy in some models of Parkinson's disease (PD) and represent a promising novel class of disease modifying therapeutics for neurodegeneration. [1, 2, 3] Efforts to develop potent and selective therapies that mitigate LRRK2-hyperactivation associated with pathogenic *LRRK2* mutations have recently intensified in industry. [4, 5] Reliable measures of LRRK2 expression and enzymatic inhibition may assist in the identification of the most efficacious LRRK2-targeting therapies at optimized doses, particularly in early clinical trials. As some LRRK2-targeting molecules have recently progressed through initial safety trials,[6] non-invasive pharmacodynamic measures in biofluids may be valuable to establish on-target drug effects in the brain (i.e., LRRK2 kinase inhibition or reduction in total protein levels). With renewed emphasis on precision approaches in the clinic, comprehensive demonstrations of robust target engagement during initial safety trials (e.g., in acute ascending dose strategies) may help successfully identify the best molecules to transition to larger efficacy studies in limited populations of genetically-defined LRRK2-linked PD. [5, 7, 8]

LRRK2 is a phospho-protein in all cells and tissues so-far evaluated,[9] with a cluster of phosphorylated residues controlled by several other kinases and phosphatases that can regulate LRRK2 interactions with 14-3-3 proteins. [10, 11, 12] Small molecule LRRK2 kinase inhibitors acutely reduce constitutive phospho-sites in LRRK2, most notably pS935,[10, 12] as well as the autophosphorylated residue pS1292 located in the C-terminal region of the LRRK2 leucine-rich repeat (LRR) domain.[13, 14, 15] LRRK2 robustly autophosphorylates its own Rab-like GTPase domain *in vitro*,[16, 17, 18] in addition to phosphorylating other GTP-bound Rab proteins (i.e., Rab10) both *in vitro* and *in vivo*.[19, 20] LRRK2 kinase inhibitors reduce levels of phospho-Rab10 in *ex vivo* inhibitor treatments of immune cells that express high levels of LRRK2 protein (e.g., monocytes, neutrophils, and whole-lysates of mononuclear cells), as well as in tissues (e.g., lung and kidney) procured from mice and rats.[21, 22, 23] pS1292-LRRK2 and pT73-Rab10 are direct substrates of LRRK2, although the phosphatases that affect these sites are likely different in cells and tissues potentially affecting pharmacodynamic marker kinetics.[24] Apart from protein pharmacodynamic markers, levels of di-docosahexaenoyl (22:6) bis (monoacylglycerol) phosphate (di-22:6-BMP) which are usually elevated in phospholipidosis and lysosomal storage

diseases,[25, 26, 27] are decreased in urine from LRRK2-inhibitor treated non-human primates.[28] The mechanisms behind LRRK2-inhibitor induced decreases in di-22:6-BMP in urine have yet to be fully defined.

Recently we identified LRRK2 protein secreted by cells in a type of microvesicle called exosomes that are derived from multivesicular bodies.[29] Although only a small fraction of LRRK2 protein is secreted into exosomes, the ratio of phospho-LRRK2 to total LRRK2 levels appears comparable between exosome and total cell (or tissue) lysates.[13] The exosome fraction of biofluids (sometimes called liquid-biopsies) allows the assessment of cellular levels of proteins from tissues that are otherwise inaccessible for analysis, for example the brain. LRRK2 protein is widely expressed through the body, with inducible expression in some immune cell subsets with pro-inflammatory agonists, and constitutive tissue expression in some cells in the brain, lung, and kidney.[5, 28, 30, 31, 32] In some model systems, LRRK2 kinase inhibitors, usually in great excess of binding affinity concentrations, can reduce total LRRK2 protein levels comparably to effects seen with anti-sense LRRK2-targeting oligonucleotides.[33, 34] The reduction of total LRRK2 protein in cells and tissues may relate to how specific inhibitors interact in the ATP-pocket, whereas LRRK2 inhibitor-induced reductions in exosome secretion in biofluids may relate to LRRK2 subcellular localization changes in the endolysosomal compartment broadly caused by kinase inhibition.[23, 29, 35, 36] Although phospho-LRRK2 to total-LRRK2 ratios have been suggested as efficacious measures of LRRK2 inhibitors,[10] inhibitor-induced destabilization of LRRK2 protein or reductions of secreted LRRK2 protein may confound interpretation of these ratios.

Biochemical surveys of LRRK2 kinase activity in *ex vivo* assays of proteins purified from mouse-derived cells and tissues reveal much higher LRRK2 activity in the brain than in other tissues and cells.[37] Further, autophosphorylated LRRK2 protein (i.e., pS1292-LRRK2) appears particularly high in human CSF exosomes as compared to exosomes procured from human urine or lysates of immune cells.[13] As a novel potential clinical target for neurodegeneration, the ostensibly desired effect of LRRK2-directed therapies centers on robust inhibition of brain clinically-accessible pharmacodynamic biomarkers that measure brain LRRK2 inhibition. Such markers are therefore sought after but have not been previously described. Herein we better define the relationship between LRRK2 inhibition and different proposed pharmacodynamic

markers, focusing on the clinically available biofluids blood, urine, and CSF. We employ structurally distinct, orally available, highly potent (low-to-sub nanomolar-binding), highly-selective, small molecule LRRK2 kinase inhibitors PFE-360, MLi2, and RA283.[23, 38] The use of non-human primates that have pharmacokinetic responses more similar to humans compared to rodents further allows the collection of sufficient volumes of urine and CSF for LRRK2 detection at the same time as blood collections to identify predictive markers of LRRK2 inhibition with the potential for translation to human studies.

Results

To measure pharmacodynamic responses related to LRRK2 kinase inhibition in macaques, PBMCs, plasma, urine, and CSF were procured from ten animals prior to drug administration. Two groups of five macaques were then treated daily with either 5 mg kg^{-1} of PFE-360 or MLi2 (Supplemental Figure 1A, B). On the fifth day of treatment, PBMCs, plasma, urine, and CSF were collected two hours after the final drug dose to allow for a range of nanomolar plasma concentrations of unbound drug. Concentrations of PFE-360 varied in the five macaques at the time of collection from ~40 nM to ~145 nM. Plasma concentrations of MLi2 varied between ~12 nM and ~70 nM. No adverse drug reactions were noted in any animal.

Blood markers of LRRK2 kinase inhibition

LRRK2 is differentially expressed in immune cells in PBMCs, with some of the highest LRRK2 expression in monocytes, B-cells, and neutrophils.[31, 39, 40, 41] Compared to the baseline levels of total LRRK2 in PBMCs, PFE-360 treatment caused a large drop in LRRK2 levels (normalized to β-actin, unadjusted for immune cell subtypes), with just 22% average of total LRRK2 protein remaining ($Mdn_{PFE\text{-}360}$= 0.15, IQR= 0.07- 0.27, $t(4)$= 9.45, p=.0007), and undetectable quantities of pS935-LRRK2 (Figure 1 and Supplemental Figure 2A). The LRRK2 autophosphorylation site pS1292-LRRK2, detectable in human CSF and urinary exosomes in past studies,[13, 42, 43, 44] was not reliably detected in PBMC lysates. Total Rab10 levels, also normalized to β-actin and unadjusted for immune cell subtypes, were variable in expression in PBMCs ($Mdn_{PFE\text{-}360}$= 1.07, IQR= 1.03- 1.34, $t(4)$= 1.37, p=.24, Figure 1D). Four of five macaques demonstrated a reduction in pT73-Rab10 levels ($Mdn_{PFE\text{-}360}$= 0.12, IQR= 0.06- 0.42, Figure 1E, F). One outlying macaque had baseline levels of pT73-Rab10 that fell below our limit of detection (Supplemental Figure 2A, lane 1) and was excluded. Plasma levels of the phospholipid di-22:6-BMP were not reduced

through PFE-360 treatments and varied in concentration, with an average of 8.07 ± 2.35 ng mL^{-1} at baseline and 7.50 ± 3.70 ng mL^{-1} after treatment.

In MLi2 treated macaques, total LRRK2 protein also diminished in PBMC pellets normalized to β-actin concentrations (Mdn_{MLi2}= 0.57, IQR= 0.40- 0.88 $t(4)$=4.38, p= .01), but to a lesser extent than PFE-360, 47% diminished compared to 78% with PFE-360 on average (Figure 1A and Supplemental Figure 2B), consistent with our past experience with these drugs in rats and mice.[23] pS935-LRRK2 signal was detected in all MLi2-treated macaques at low levels compared to baseline (Mdn_{MLi2}= 0.11, IQR= 0.06- 0.26, $t(4)$= 3.98, p=.02), although one macaque showed only a 50% reduction in pS935-LRRK2 that also had the lowest concentration of unbound plasma MLi2 (12.5 nM, Figure 1H). pT73-Rab10 levels reduced by 71% on average (Mdn_{MLi2}= 0.39, IQR= 0.06- 0.63, $t(4)$= 4.35, p=.01, Figure 1E), even in the macaque with just 12.5 nM of drug in circulation. The ratio of pT73-Rab10 to total Rab10 protein offered a comparable indication to pT73-Rab10 measures alone (Mdn_{MLi2}= 0.16, IQR= 0.02- 0.20, $t(4)$= 3.85, p=.02, Figure 1F, J). Overall these results suggest that pS935-LRRK2 and pT73-Rab10 levels are reliably reduced when normalized to β-actin in PBMCs after LRRK2 kinase inhibitor treatment, whereas total LRRK2 levels and total Rab10 levels were more variably affected.

Urine markers of LRRK2 kinase inhibition

Our previous work localized LRRK2 protein expression in urine to urinary exosomes.[42, 43, 44] Compared to baseline measures of LRRK2 in macaque urinary exosomes, PFE-360 or MLi2 treatment caused a profound decrease in several NHPs in total LRRK2 protein normalized to the exosome house-keeping protein TSG101 ($Mdn_{PFE-360}$= 0.04, IQR= 0- 0.64, $t(4)$= 2.66, p=.06; Mdn_{MLi2}= 0.02, IQR= 0.01- 0.11, $t(4)$= 2.15, p=.10, Figure 2A and Supplemental Figure 3). A comparable decrease was noted with pS935-LRRK2 protein ($Mdn_{PFE-360}$= 0.21, IQR= 0.01- 0.43, $t(4)$= 2.84, p=.05; Mdn_{MLi2}= 0, IQR= 0- 0.04, $t(4)$= 2.15, p=.10, Figure 2B and Supplemental Figure 3). Owing to the reductions in total LRRK2 protein caused by kinase inhibition, the ratio of pS935-LRRK2 to total LRRK2 protein was much more variable in drug-responses, especially in NHPs where total LRRK2 protein was most dramatically reduced (Figure 2C). The LRRK2 autophosphorylation site pS1292 was not reliably detected in macaque urine. Total Rab10 levels, also normalized to the exosome housekeeper TSG101, was more variable than LRRK2 levels, with 3 of 5 PFE-360-treated and 4 of 5 MLi2-treated macaques showing decreases in total Rab10

($Mdn_{PFE-360}$= 0.50, IQR= 0.41- 2.31, $t(4)$= 0.10, p=.92; Mdn_{MLi2}= 0.27, IQR= 0.14- 0.56, $t(4)$= 2.03, p=.11, Figure 1D). Further decreases, albeit nominal compared to total LRRK2 decreases, were observed with pT73-Rab10 in most macaques ($Mdn_{PFE-360}$= 0.28, IQR= 0.15- 1.54, $t(4)$= 2.25, p=.09; Mdn_{MLi2}= 0.12, IQR= 0.08- 0.25, $t(4)$= 3.30, p=.03, Figure 1E). The ratio of pT73-Rab10 to total Rab10 protein decreased in the macaques with the highest plasma concentrations of PFE-360 (~145 nM, 50% remaining from baseline, $Mdn_{PFE-360}$= 0.43, IQR= 0.30- 0.71, $t(4)$= 3.46, p=.03) and MLi2 (~70 nM, 30% remaining from baseline, Mdn_{MLi2}= 0.60, IQR= 0.31- 0.75, $t(4)$= 2.70, p=.05, Figure 2F, G, H). Overall, PFE-360 and MLi2 treatment consistently reduced total LRRK2 protein secretion in urinary exosomes. As with PBMC analyses, ratios of phospho- to total protein as a pharmacodynamic measure could be considered confounded due to variable changes of total protein levels.

Previous studies demonstrated that the phospholipid di-22:6-BMP, usually strongly elevated in phospholipidosis,[25, 26, 45] is reduced in the urine of LRRK2 knockout mice and non-human primates treated with the LRRK2 inhibitor GNE-7915.[28] We wondered whether the same effect could be obtained in exosome-depleted urine used for simultaneous measures of exosomal-LRRK2 protein. We measured di-22:6-BMP levels normalized to urine creatinine in the exosome-depleted urine, with baseline concentrations of di-22:6-BMP equal to 12.8 ± 9.18 ng per mg of creatinine. One macaque demonstrated very high baseline levels of di-22:6-BMP in the MLi2-treated group (~100 ng, Figure 2I). With LRRK2 inhibitor treatment, di-22:6-BMP levels in the exosome-depleted urine dropped to near undetectable levels in the PFE-360 condition ($Mdn_{PFE-360}$=0.05, IQR= 0.01- 0.07, $t(4)$= 2.69, p=.05). In the MLi2 group, one macaque had very low levels of di-22:6-BMP at baseline in exosome-depleted urine (~1 ng) and had the lowest concentration of MLi2 in plasma (12.5 nM) as well as heightened Rab10 levels in PBMCs. Exclusion of the animal with low levels of unbound MLi2 and lack of LRRK2 inhibition in PBMCs revealed a similar trend of reduced di-22:6-BMP in exosome-depleted urine with MLi2 treatment (p<0.01, Figure 2I). Concentrations of di-22:6-BMP were not measured in the total urine specimens (i.e., prior to exosome depletion), in the isolated urine exosomes, or adjusted by exosome-depletion efficiency in individual samples. Overall, reduced di-22:6-BMP was observed in exosome-depleted urine with LRRK2 inhibitor treatment, consistent with exosomal-LRRK2 protein depletion measures.

Cerebrospinal fluid markers of LRRK2 kinase inhibition

Our previous work in biobanked human CSF demonstrated that LRRK2 protein and pS1292-LRRK2 protein can be readily measured in exosome fractions.[13] In exosomes isolated from human CSF, LRRK2 autophosphorylation at the serine 1292 residue is much higher (~5-fold increased on average), as opposed to urinary exosomes from the same subjects.[13] In macaque CSF exosomes, total LRRK2 levels diminished with PFE-360 treatment ($Mdn_{PFE\text{-}360}$=0.09, IQR= 0.03- 0.44, $t(4)$= 4.07, p=.02), as well as pS1292-LRRK2 levels ($Mdn_{PFE\text{-}360}$=0.01, IQR= 0.001-0.13, $t(4)$= 3.14, p=.03). Both markers were normalized to the exosome housekeeping protein Flotillin-1 (Figure 3A,B and Supplemental Figure 4A).

Following MLi2 treatment, total LRK2 levels in CSF exosomes were reduced by 35% compared to baseline (Mdn_{MLi2}=0.67, IQR= 0.28- 1.39, $t(4)$= 2.98, p=.04, Figure 3A). Treatment with MLi2 revealed an exposure-sensitive decrease in pS1292-LRRK2 (Mdn_{MLi2}=0.30, IQR= 0.11-1.51, $t(4)$= 3.56, p=.02, Figure 3B, D and Supplemental Figure 4C). In CSF exosome lysates from all samples, pT73-Rab10 and total Rab10 could not be detected. The levels of di-22:6-BMP in the exosome-depleted CSF were not changed with PFE-360 treatment or with MLi2 treatment (Supplemental Figure 4B, D). However, the reliability of the results could be confounded due to variable exosome depletion in individual samples. As with urine analyses, concentrations of di-22:6-BMP were not measured in the total CSF specimens (i.e., prior to exosome depletion) or in the isolated CSF exosomes due to CSF volume limitations in this study.

LRRK2 kinase inhibition lowers exosome LRRK2 in CSF

In past work in rats and mice, PFE-360 treatment partially reduced total LRRK2 levels in brain tissue at lower concentrations than MLi2, despite similar cell potencies and pharmacokinetics of the drugs.[23] To better resolve the relationship between brain LRRK2 kinase inhibition and LRRK2 secretion in urinary and CSF exosomes, we tested a third structurally distinct LRRK2 kinase inhibitor, known as RA283, in a low-dose group and a high-dose group (10 and 30 mg kg^{-1}, respectively) compared to a vehicle only-treated group. Macaques were treated (vehicle, low-dose, or high-dose) for a week and killed for the analysis of brain tissue collected at the same time as blood, urine, and CSF to explore the relationship of these fluid markers with inhibition of LRRK2 in brain tissue.

Similar to PFE-360 treatments, RA283 treatment reduced total exosome LRRK2 protein levels in the CSF in three of four treated macaques (Figure 4 and Supplemental Figure 5). Analysis of PBMCs showed a strong reduction of total LRRK2 levels in both low-dose and high-dose treated animals compared to vehicle-control animals (Figure 4 and Supplemental Figure 6). pS935-LRRK2 levels were nearly ablated at unbound drug plasma concentrations that ranged from ~3 nM to 17 nM (Figure 4B). Consistent with PFE-360 and MLi2 results, a near complete ablation of total LRRK2 protein levels was noted in urinary exosomes at higher plasma drug concentrations (Figure 4C). Evaluation of cortical brain tissue revealed lower total-LRRK2 protein levels (compared to vehicle treated) only in the high-dose animals (Figure 4E). It is worth noting that both doses led to reduced pS935-LRRK2 levels in brain tissue (~43% at lowest dose and ~87% at highest dose, Figure 4F). Thus, these results demonstrate partial inhibition of LRRK2 kinase activity in brain tissue can lead to a near-complete ablation of total LRRK2 protein levels (and pS1292-LRRK2 protein) in CSF exosomes. These results are consistent with past studies in cell culture suggesting LRRK2-protein release in exosomes is sensitive to kinase inhibition potentially through blocking chaperone activity of 14-3-3.[29]

Discussion

This study identifies effective quantitative measures for LRRK2 kinase inhibition in biofluids (urine and CSF) of non-human primates using three structurally distinct small-molecules (PFE-360, MLi2, and RA283). All three molecules have very high potency in blocking LRRK2 kinase activity in NHPs and excellent drug-properties for the study, yet differences emerged in inhibition profiles with different pharmacodynamic measures in PBMCs, urine, and CSF. While the current standard in the field may be to determine the ratio of phospho-LRRK2 protein to total LRRK2 protein to estimate LRRK2 kinase inhibition, our results here demonstrate that this measure may be critically confounded due to variable decreases in total LRRK2 that can be differentially influenced by distinct classes of small molecules. A trend emerged here, consistent with our past studies in transfected cell lines,[29] mice, and rats,[23] where exosome levels of total LRRK2 protein diminish prior to LRRK2-inhibitor induced decreases in brain tissue (graphically summarized in Figure 5A). In practice, determining LRRK2 inhibitor target engagement in CSF-derived exosomes revealed a similar profile of total LRRK2 protein reduction to that of the autophosphorylated LRRK2 protein (results summarized in Figure 5B).

In past studies, we, and others, demonstrated elevated LRRK2-autophosphorylation and LRRK2 protein levels associated with PD susceptibility and LRRK2 pathogenic mutations.[13, 43, 46] With high endogenous LRRK2 expression in some types of innate immune cells, PBMCs have been championed as a source for pharmacodynamic biomarkers related to LRRK2 inhibition,[47] and are currently utilized in clinical trials. However, measures in PBMCs alone may poorly predict LRRK2 inhibition in the brain and other tissues, for example with drugs that are poorly brain penetrant or are rapidly eliminated. Further, PBMCs rapidly turn over and transiently respond to diverse stimuli. Ideally, we suggest that combinations of predictive markers that assess LRRK2 inhibition and pharmacodynamic responses across the body will better highlight the most efficacious drugs and dosage regimens. Past studies with drugs like azidothymidine demonstrate that measurements of drug concentration in CSF do not predict brain penetration of the drug and target engagement in the brain.[48, 49] We suggest that measuring CSF levels of LRRK2 protein in exosomes could contribute to establishing brain penetration in early phase clinical trials (e.g., acute safety studies).

In past work with different LRRK2 pharmacodynamic measures, despite robust results in analyzing tissues (i.e., brain, lung, kidney [23]), we have been unable to reliably detect LRRK2 or Rab proteins in urine or CSF procured from rats or mice. The limited biofluids volume obtained from rats and mice compared to NHP appear not to be the reason since we would pool biofluids in excess of volumes studied here. While the reasons behind our limited success in rodents are not clear, we were able to establish robust measures in NHP urine and CSF to profile LRRK2 kinase inhibitors. Pairs of successful markers in each biofluids included pS935-LRRK2 and pT73-Rab10levels measured in PBMCs, total LRRK2 and di-22:6-BMP levels measured in urine exosomes and exosome-depleted urine, respectively, and levels of total LRRK2 and pS1292-LRRK2 measured in CSF exosomes. It is plausible that the inhibition profile of each drug would further change under different dosages or time intervals post-oral gavage, or in a chronic inhibition study such as an efficacy trial in the clinic. Nevertheless, we would predict this panel of markers would be capable of identifying drugs that poorly inhibit LRRK2 in the brain but effectively inhibit LRRK2 in the periphery, for example a drug that may cause differential changes in PBMC and urine markers but not in CSF markers. A further critical test of this hypothesis could involve a LRRK2 kinase inhibitor series that can be modified to either efficiently cross the blood brain barrier or be excluded from the brain. It will be critical to the

success of new compounds to utilize these types of assays in early phase clinical trials to ensure sufficient target engagement in the brain. Many new compounds have high attrition rates due to presumed lack of target engagement at doses resolved in safety studies.[50] Implementing biomarker target engagement early may help improve drug development outcomes.

Pathogenic mutations in LRRK2 are now recognized as one of the most common genetic causes of neurodegeneration, and these mutations all appear to result in LRRK2 kinase hyper-activation.[5, 51, 52] Emerging studies also suggest a proportion of idiopathic PD that share hyper-activated LRRK2 phenotypes.[40, 43, 53, 54, 55] Several small-molecule LRRK2 kinase inhibitors and anti-sense oligonucleotides have been evaluated for efficacy and safety in various model systems, including non-human primates.[1, 3, 28, 34, 38, 47] Many if not most therapeutics that target central nervous-system indications move to clinical trials without convincing biomarkers for target engagement. Yet, the use of reliable biomarkers has been shown to increase the chance of success in the clinic.[56, 57] As potential LRRK2-targeting therapeutics like small molecule LRRK2 kinase inhibitors and LRRK2-targeting anti-sense oligonucleotides move forward, there is an acute need for validated pharmacodynamic and theragnostic markers to monitor the success of different classes of LRRK2 kinase inhibitors in blocking LRRK2 activity associated with disease. Notably, the protein measurement assays presented here are based on immunoblotting procedures that, while linear and quantitative in our protocols,[13] do not scale well into clinically available tests. Further assay development will be needed for broad clinical implementation.

Here, our data suggest that measures of pS935-LRRK2 and pT73-Rab10, each normalized to β-actin, represent blood biomarkers of target engagement. PBMCs are easily procured in the clinic and provide a reliable resource for measuring LRRK2 inhibition in circulating cells. Several studies have shown high LRRK2 expression in specific immune cell subsets.[5, 31, 32, 39, 41, 58] Immunophenotyping blood from PD patients shows increased LRRK2 expression in monocytes and B-cells compared to healthy controls.[40, 54] *Ex vivo* treatment of PBMCs with LRRK2 kinase inhibitors result in a reduction of the constitutive LRRK2 phosphorylation site pS935-LRRK2 without acute toxicity.[59] While we can reproduce the reduction (e.g., with MLi2 treatment) or complete ablation (e.g., with PFE-360 treatment) of pS935-LRRK2, total LRRK2 levels are variably affected in PBMCs that may confound the interpretation of the ratio of phosphorylated to unphosphorylated peptide. We observe the same confounding issue with Rab10, presumably

due to changes in protein turnover with phosphorylation as well as inducible expression in immune cell subtypes that may change with kinase inhibition over time, at least in NHPs.

Urine can be obtained non-invasively and in higher abundance than other biofluids, at least in humans.[13] Our recent proteomics studies suggest urinary exosomes harbor cytosolic proteins that demarcate organs across the body without enrichment of kidney proteins.[44] Exosomal LRRK2 is both dimerized and phosphorylated, mimicking cytosolic active isoforms.[29, 60, 61] LRRK2 kinase inhibitors reduced LRRK2 protein secretion in urinary exosomes, whereas pT73-Rab10 decreased in an exposure-dependent manner. Di-22:6-BMP, a biomarker of lysosomal dysregulation, was reduced in exosome-depleted urine with LRRK2 inhibitor treatment. These results were consistent with past observations of other structurally distinct LRRK2 kinase inhibitors in NHPs.[28] The observed decrease in di-22:6-BMP was similar to that observed in LRK2 KO mice, and shown to decrease with pS935-LRRK2 and pT73-Rab10 in lysates from brain, kidney, lung, and PBMCs.[19] A consequence of LRRK2 inhibition would be the decreased phosphorylation of its Rab GTPase substrates and thereby their accumulation in membranes.[14, 62] We propose that the shift in membrane-bound Rabs may affect the biogenesis, motility, and/or transport of BMP containing vesicles (e.g., exosomes, secretory lysosomes) outside of the cell, resulting in the observed decrease in BMP in the urine.[63] Although its source(s) remain unclear (i.e., BMPs are found in a variety of tissues and cell types, including brain), reported changes in urinary di-22:6-BMP appear to reflect a LRRK2-driven effect on lysosomal and secretory biology.[64]

Consistent with our previous studies in cell lines, [29] we predict that LRRK2 inhibition manifests in biofluids first with the reduction of LRRK2 protein that is secreted in exosomes and, at higher drug doses or subsequent to a strong sustained exposure, manifests with reductions in total cellular levels of LRRK2 protein (illustrated in Figure 5A). We propose that 14-3-3 chaperones LRRK2 protein to multivesicular bodies that export LRRK2 in exosomes, and this interaction becomes rapidly disrupted at lower doses of LRRK2 kinase inhibitors than those required for destabilizing LRRK2 protein in total. Our data here show that this relationship can be harnessed for effective LRRK2 target engagement assays in blood, urine, and CSF. Overall, we hope these results help provide a path to establish on-target effects of LRRK2-targeting investigational

therapeutics in both the periphery and the CNS in clinical populations to improve the chances of a successful clinical trial.

References

1. Daher, J.P. *et al.* Leucine-rich Repeat Kinase 2 (LRRK2) Pharmacological Inhibition Abates alpha-Synuclein Gene-induced Neurodegeneration. *The Journal of biological chemistry* **290**, 19433-19444 (2015).

2. Zhao, H.T. *et al.* LRRK2 Antisense Oligonucleotides Ameliorate α-Synuclein Inclusion Formation in a Parkinson's Disease Mouse Model. *Mol Ther Nucleic Acids* **8**, 508-519 (2017).

3. Volpicelli-Daley, L.A. *et al.* G2019S-LRRK2 Expression Augments alpha-Synuclein Sequestration into Inclusions in Neurons. *The Journal of neuroscience : the official journal of the Society for Neuroscience* **36**, 7415-7427 (2016).

4. Alessi, D.R. & Sammler, E. LRRK2 kinase in Parkinson's disease. *Science* **360**, 36 (2018).

5. West, A.B. Achieving neuroprotection with LRRK2 kinase inhibitors in Parkinson disease. *Experimental Neurology* **298**, 236-245 (2017).

6. Therapeutics, D. Denali Therapeutics Announces Positive Clinical Results From LRRK2 Inhibitor Program For Parkinson's Disease. 2018 [cited 2019 August 1st]Available from: http://investors.denalitherapeutics.com/news-releases/news-release-details/denali-therapeutics-announces-positive-clinical-results-lrrk2

7. Ivy, S.P., Siu, L.L., Garrett-Mayer, E. & Rubinstein, L. Approaches to Phase 1 Clinical Trial Design Focused on Safety, Efficiency, and Selected Patient Populations: A Report from the Clinical Trial Design Task Force of the National Cancer Institute Investigational Drug Steering Committee. *Clinical Cancer Research* **16**, 1726 (2010).

8. Sistare, F.D. *et al.* Towards consensus practices to qualify safety biomarkers for use in early drug development. *Nature Biotechnology* **28**, 446-454 (2010).

9. West, A.B. *et al.* Parkinson's disease-associated mutations in LRRK2 link enhanced GTP-binding and kinase activities to neuronal toxicity. *Hum Mol Genet* **16**, 223-232 (2007).

10. Dzamko, N. *et al.* Inhibition of LRRK2 kinase activity leads to dephosphorylation of Ser(910)/Ser(935), disruption of 14-3-3 binding and altered cytoplasmic localization. *Biochem J* **430**, 405-413 (2010).

11. Li, X. *et al.* Phosphorylation-Dependent 14-3-3 Binding to LRRK2 Is Impaired by Common Mutations of Familial Parkinson's Disease. *PLOS ONE* **6**, e17153 (2011).

12. Nichols, R.J. *et al.* 14-3-3 binding to LRRK2 is disrupted by multiple Parkinson's disease-associated mutations and regulates cytoplasmic localization. *Biochemical Journal* **430**, 393 (2010).

13. Wang, S. *et al.* Elevated LRRK2 autophosphorylation in brain-derived and peripheral exosomes in LRRK2 mutation carriers. *Acta neuropathologica communications* **5**, 86 (2017).

14. Liu, Z. *et al.* LRRK2 phosphorylates membrane-bound Rabs and is activated by GTP-bound Rab7L1 to promote recruitment to the trans-Golgi network. *Hum Mol Genet* **27**, 385-395 (2018).

15. Henry, A.G. *et al.* Pathogenic LRRK2 mutations, through increased kinase activity, produce enlarged lysosomes with reduced degradative capacity and increase ATP13A2 expression. *Hum Mol Genet* **24**, 6013-6028 (2015).

16. Greggio, E. *et al.* The Parkinson's disease kinase LRRK2 autophosphorylates its GTPase domain at multiple sites. *Biochemical and biophysical research communications* **389**, 449-454 (2009).

17. Muda, K. *et al.* Parkinson-related LRRK2 mutation R1441C/G/H impairs PKA phosphorylation of LRRK2 and disrupts its interaction with 14-3-3. *Proceedings of the National Academy of Sciences of the United States of America* **111**, E34-43 (2014).

18. Liu, Z., Mobley, J.A., DeLucas, L.J., Kahn, R.A. & West, A.B. LRRK2 autophosphorylation enhances its GTPase activity. *FASEB journal : official publication of the Federation of American Societies for Experimental Biology* **30**, 336-347 (2016).

19. Steger, M. *et al.* Phosphoproteomics reveals that Parkinson's disease kinase LRRK2 regulates a subset of Rab GTPases. *eLife* **5** (2016).

20. West, A.B. & Cookson, M.R. Identification of bona-fide LRRK2 kinase substrates. *Movement disorders : official journal of the Movement Disorder Society* **31**, 1140-1141 (2016).

21. Lis, P. *et al.* Development of phospho-specific Rab protein antibodies to monitor in vivo activity of the LRRK2 Parkinson's disease kinase. *Biochem J* **475**, 1-22 (2018).

22. Fan, Y. *et al.* Interrogating Parkinson's disease LRRK2 kinase pathway activity by assessing Rab10 phosphorylation in human neutrophils. *Biochem J* **475**, 23-44 (2018).

23. Kelly, K. *et al.* The G2019S mutation in LRRK2 imparts resiliency to kinase inhibition. *Experimental Neurology* **309**, 1-13 (2018).

24. Berndsen, K. *et al.* PPM1H phosphatase counteracts LRRK2 signaling by selectively dephosphorylating Rab proteins. *eLife* **8** (2019).

25. Tengstrand, E., Zhang, H., Liu, N., Dunn, K. & Hsieh, F. A multiplexed UPLC-MS/MS assay for the simultaneous measurement of urinary safety biomarkers of drug-induced kidney injury and phospholipidosis. *Toxicology and applied pharmacology* **366**, 54-63 (2019).

26. Liu, N., Tengstrand, E.A., Chourb, L. & Hsieh, F.Y. Di-22:6-bis(monoacylglycerol)phosphate: A clinical biomarker of drug-induced phospholipidosis for drug development and safety assessment. *Toxicology and applied pharmacology* **279**, 467-476 (2014).

27. Meikle, Peter J. *et al.* Effect of lysosomal storage on bis(monoacylglycero)phosphate. *Biochemical Journal* **411**, 71 (2008).

28. Fuji, R.N. *et al.* Effect of selective LRRK2 kinase inhibition on nonhuman primate lung. *Sci Transl Med* **7**, 273ra215 (2015).

29. Fraser, K.B. *et al.* LRRK2 secretion in exosomes is regulated by 14-3-3. *Hum Mol Genet* **22**, 4988-5000 (2013).

30. Biskup, S. *et al.* Dynamic and redundant regulation of LRRK2 and LRRK1 expression. *BMC Neuroscience* **8**, 102 (2007).

31. Hakimi, M. *et al.* Parkinson's disease-linked LRRK2 is expressed in circulating and tissue immune cells and upregulated following recognition of microbial structures. *Journal of Neural Transmission* **118**, 795-808 (2011).

32. Maekawa, T., Kubo, M., Yokoyama, I., Ohta, E. & Obata, F. Age-dependent and cell-population-restricted LRRK2 expression in normal mouse spleen. *Biochemical and biophysical research communications* **392**, 431-435 (2010).

33. Skibinski, G., Nakamura, K., Cookson, M.R. & Finkbeiner, S. Mutant LRRK2 toxicity in neurons depends on LRRK2 levels and synuclein but not kinase activity or inclusion bodies. *The Journal of neuroscience : the official journal of the Society for Neuroscience* **34**, 418-433 (2014).

34. Zhao, H.T. *et al.* LRRK2 Antisense Oligonucleotides Ameliorate alpha-Synuclein Inclusion Formation in a Parkinson's Disease Mouse Model. *Mol Ther Nucleic Acids* **8**, 508-519 (2017).

35. De Wit, T., Baekelandt, V. & Lobbestael, E. Inhibition of LRRK2 or Casein Kinase 1 Results in LRRK2 Protein Destabilization. *Molecular neurobiology* **56**, 5273-5286 (2019).

36. Lobbestael, E. *et al.* Pharmacological LRRK2 kinase inhibition induces LRRK2 protein destabilization and proteasomal degradation. *Sci Rep* **6**, 33897 (2016).

37. Li, X. *et al.* Enhanced Striatal Dopamine Transmission and Motor Performance with LRRK2 Overexpression in Mice Is Eliminated by Familial Parkinson's Disease Mutation G2019S. *The Journal of Neuroscience* **30**, 1788 (2010).

38. Fell, M.J. *et al.* MLi-2, a Potent, Selective, and Centrally Active Compound for Exploring the Therapeutic Potential and Safety of LRRK2 Kinase Inhibition. *J Pharmacol Exp Ther* **355**, 397-409 (2015).

39. Thévenet, J., Pescini Gobert, R., Hooft van Huijsduijnen, R., Wiessner, C. & Sagot, Y.J. Regulation of LRRK2 Expression Points to a Functional Role in Human Monocyte Maturation. *PLOS ONE* **6**, e21519 (2011).

40. Cook, D.A. *et al.* LRRK2 levels in immune cells are increased in Parkinson's disease. *npj Parkinson's Disease* **3**, 11 (2017).

41. Kubo, M. *et al.* LRRK2 is expressed in B-2 but not in B-1 B cells, and downregulated by cellular activation. *Journal of neuroimmunology* **229**, 123-128 (2010).

42. Fraser, K.B., Moehle, M.S., Alcalay, R.N., West, A.B. & Consortium, L.C. Urinary LRRK2 phosphorylation predicts parkinsonian phenotypes in G2019S LRRK2 carriers. *Neurology* **86**, 994-999 (2016).

43. Fraser, K.B. *et al.* Ser(P)-1292 LRRK2 in urinary exosomes is elevated in idiopathic Parkinson's disease. *Movement Disorders* **31**, 1543-1550 (2016).

44. Wang, S., Kojima, K., Mobley, J.A. & West, A.B. Proteomic analysis of urinary extracellular vesicles reveal biomarkers for neurologic disease. *EBioMedicine* **45**, 351-361 (2019).

45. Tengstrand, E.A., Miwa, G.T. & Hsieh, F.Y. Bis(monoacylglycerol)phosphate as a non-invasive biomarker to monitor the onset and time-course of phospholipidosis with drug-induced toxicities. *Expert Opinion on Drug Metabolism & Toxicology* **6**, 555-570 (2010).

46. Fraser, K.B., Moehle, M.S., Alcalay, R.N. & West, A.B. Urinary LRRK2 phosphorylation predicts parkinsonian phenotypes in G2019S LRRK2 carriers. *Neurology* **86**, 994-999 (2016).

47. Thirstrup, K. *et al.* Selective LRRK2 kinase inhibition reduces phosphorylation of endogenous Rab10 and Rab12 in human peripheral mononuclear blood cells. *Sci Rep* **7**, 10300 (2017).

48. Pardridge, W.M. Drug transport in brain via the cerebrospinal fluid. *Fluids and Barriers of the CNS* **8**, 7 (2011).

49. Dykstra, K.H. *et al.* Microdialysis study of zidovudine (AZT) transport in rat brain. *J Pharmacol Exp Ther* **267**, 1227-1236 (1993).

50. Morgan, P. *et al.* Can the flow of medicines be improved? Fundamental pharmacokinetic and pharmacological principles toward improving Phase II survival. *Drug discovery today* **17**, 419-424 (2012).

51. West, A.B. Ten years and counting: moving leucine-rich repeat kinase 2 inhibitors to the clinic. *Movement Disorders* **30**, 180-189 (2015).

52. Cookson, M.R. The role of leucine-rich repeat kinase 2 (LRRK2) in Parkinson's disease. *Nature reviews. Neuroscience* **11**, 791-797 (2010).

53. Gilks, W.P. *et al.* A common LRRK2 mutation in idiopathic Parkinson's disease. *The Lancet* **365**, 415-416 (2005).

54. Bliederhaeuser, C. *et al.* LRRK2 contributes to monocyte dysregulation in Parkinson's disease. *Acta Neuropathol Commun* **4**, 123 (2016).

55. Di Maio, R. *et al.* LRRK2 activation in idiopathic Parkinson's disease. *Sci Transl Med* **10** (2018).

56. Lopes, G. *et al.* The role of biomarkers in improving clinical trial success: A study of 1,079 oncology drugs. *Journal of Clinical Oncology* **33**, e17804-e17804 (2015).

57. Wong, C.H., Siah, K.W. & Lo, A.W. Estimation of clinical trial success rates and related parameters. *Biostatistics (Oxford, England)* **20**, 273-286 (2019).

58. Gardet, A. *et al.* LRRK2 is involved in the IFN-gamma response and host response to pathogens. *Journal of immunology (Baltimore, Md. : 1950)* **185**, 5577-5585 (2010).

59. Perera, G., Ranola, M., Rowe, D.B., Halliday, G.M. & Dzamko, N. Inhibitor treatment of peripheral mononuclear cells from Parkinson's disease patients further validates LRRK2 dephosphorylation as a pharmacodynamic biomarker. *Scientific Reports* **6**, 31391 (2016).

60. Sen, S., Webber, P.J. & West, A.B. Dependence of leucine-rich repeat kinase 2 (LRRK2) kinase activity on dimerization. *The Journal of biological chemistry* **284**, 36346-36356 (2009).

61. Deng, X. *et al.* Characterization of a selective inhibitor of the Parkinson's disease kinase LRRK2. *Nature chemical biology* **7**, 203-205 (2011).

62. Steger, M. *et al.* Systematic proteomic analysis of LRRK2-mediated Rab GTPase phosphorylation establishes a connection to ciliogenesis. *Elife* **6** (2017).

63. Alcalay, R.N. *et al.* Higher Urine bis(Monoacylglycerol)Phosphate Levels in LRRK2 G2019S Mutation Carriers: Implications for Therapeutic Development. *Movement disorders : official journal of the Movement Disorder Society* (2019).

64. Baptista, M.A. *et al.* Loss of leucine-rich repeat kinase 2 (LRRK2) in rats leads to progressive abnormal phenotypes in peripheral organs. *PLoS One* **8**, e80705 (2013).

65. Henderson, J.L. *et al.* Discovery and preclinical profiling of 3-[4-(morpholin-4-yl)-7H-pyrrolo[2,3-d]pyrimidin-5-yl]benzonitrile (PF-06447475), a highly potent, selective, brain penetrant, and in vivo active LRRK2 kinase inhibitor. *Journal of medicinal chemistry* **58**, 419-432 (2015).

66. Scott, J.D. *et al.* Discovery of a 3-(4-Pyrimidinyl) Indazole (MLi-2), an Orally Available and Selective Leucine-Rich Repeat Kinase 2 (LRRK2) Inhibitor that Reduces Brain Kinase Activity. *Journal of medicinal chemistry* **60**, 2983-2992 (2017).

67. Fraser, K.B. *et al.* Ser(P)-1292 LRRK2 in urinary exosomes is elevated in idiopathic Parkinson's disease. *Mov Disord* **31**, 1543-1550 (2016).

Figures Legends

Figure 1. LRRK2 inhibition markers in PBMCs. Inhibition values for measures of LRRK2 and Rab10 in isolated PBMCs after five days of PFE-360 (blue) and MLi2 (red) treatment (5 mg kg^{-1} BID). Protein levels were normalized to the housekeeping protein β-actin. Fold median baseline values before and after (2-hours) treatment for **a.** Total LRRK2, **b.** pS935-LRRK2, **c.** pS935-LRRK2/Total LRRK2, **d.** Total Rab10, **e.** pT73-Rab10, and **f.** pT73-Rab10/Total Rab10. For Rab10 inhibition measures (panel d-f), one outlier sample in the PFE-360 treatment group was not included because baseline pT73-Rab10 levels fell below the limit of detection. Paired t-tests were performed to determine significance between baseline and post-drug exposures. Scatterplots of **g.** PFE-360 (nM) and total LRRK2, **h.** MLi2 (nM) and pS935-LRRK2, **i.** PFE-360 (nM) and pT73-Rab10/Total Rab10, and **j.** MLi2 (nM) and pT73-Rab10/Rab10. The dashed grey lines represent the median value with no drug (i.e., 0 nM).

Figure 2. LRRK2 inhibition markers in urine. a. Inhibition values for measures of exosomal LRRK2 and Rab10 after five days of PFE-360 (blue) and MLi2 (red) treatment (5 mg kg^{-1} BID). Proteins isolated from urinary exosomes were normalized to the exosome marker TSG101. Fold median baseline values before and post-treatment for **a.** Total LRRK2, **b.** pS935-LRRK2, **c.** pS935-LRRK2/Total LRRK2, **d.** Total Rab10, **e.** pT73-Rab10, and **f.** pT73-Rab10/Total Rab10. Paired t-tests were performed to determine significance between baseline and post-drug exposure measures for PFE-360 and MLi2, respectively. Scatterplots between unbound plasma concentrations of **g.** PFE-360 (nM) or **h.** MLi2 (nM) and inhibition of pT73-Rab10/Rab10. The dashed grey lines represent the median value with no drug. **i.** Di-22:6-BMP levels (ng mg^{-1} Creatinine) in exosome-depleted urine at baseline and post-drug exposure of PFE-360 (blue) or MLi2 (red). P-values were calculated using a paired t-test.

Figure 3. LRRK2 inhibition markers in CSF. a. Inhibition values for measures of exosomal LRRK2 after five days of PFE-360 (blue) and MLi2 (red) treatment (5 mg kg^{-1} BID). Proteins isolated from CSF exosomes were normalized to the exosome marker flotillin-1. Fold median baseline values before and post-treatment for **a.** Total LRRK2, **b.** pS1292-LRRK2. Dependent sample t-tests were performed to determine significance between baseline and post-drug exposure measures for PFE-360 and MLi2, respectively. Scatterplots between unbound plasma concentrations of **c.** PFE-360 (nM) or **d.** MLi2 (nM) and inhibition of pS1292-LRRK2/Total

LRRK2. The dashed grey lines represent the median value with no drug. P-values were calculated using a paired t-test.

Figure 4. LRRK2 inhibition in RA283 treated NHPs. Inhibition values for measures of LRRK2 in PBMCs, urine. CSF, and brain tissue (frontal cortex) after seven days of low dose (10 mg kg^{-1}, 3.4 nM and 3.1 nM) and high dose (30 mg kg^{-1}, 13.4 nM and 16.5 nM) RA283 treatment. Biofluids and brain tissue were procured from low dose and high dose NHPs two and six hours after the final dose, respectively. Samples were also collected from vehicle-control NHPs (0 nM RA283). Scatterplots between unbound plasma concentrations of RA283 and **a.** Total LRRK2 in PBMCS, **b.** pS935-LRRK2 in PBMCs, **c. T**otal LRRK2 in urinary exosomes, **d.** Total LRRK2 in CSF exosomes, **e.** Total LRRK2 in frontal-cortex tissue, and **f.** pS935-LRRK2 in frontal-cortex tissue. One missing sample in urine from a low-dose treated monkey. The dashed grey lines represent the median value with no drug.

Figure 5. Summary of LRRK2 inhibition. a. Diagram illustrating the relationship of LRRK2 protein in tissue or biofluids (i.e., exosomes) with % ATP-bound LRRK2 in increasing concentrations of ATP-competitive small molecule LRRK2 kinase inhibitors. In the model, exosome depletion of LRRK2 without lowering tissue levels of total LRRK2 is shown in yellow, whereas the green area highlights higher concentrations of drug and corresponding loss of any ATP-bound LRRK2, resulting in the depletion of LRRK2 protein in both exosomes and tissues. **b**. Depletion of total LRRK2 protein and pS1292-LRRK2 protein normalized to the CSF-exosome housekeeping protein flotillin-1. Depletion caused by PFE-360 and MLi2 treatments are relative to baseline measurements whereas RA282 is relative to vehicle-control measurements.

Materials and Methods

Compounds

Small-molecule LRRK2 kinase inhibitors PFE-360, MLi2, and RA283, were synthesized in-house. The identity and high purity (i.e., >97.4% for each compound) of each compound was confirmed by nuclear-magnetic resonance and mass spectrometry. PFE-360 was originally discovered as part of a Pfizer chemistry program [65], MLi2 was originally discovered as part of a Merck chemistry program [38, 66], and RA283 was discovered as part of a Sanofi chemistry program. These compounds have structurally distinct pharmacophores [65, 66] (Supplemental Figure 1).

In vitro kinase assays show similar IC_{50} potencies with the three structurally distinct inhibitors, with PFE-360 demonstrating 6 nM IC_{50} inhibition for LRRK2 autophosphorylation, MLi2 demonstrating 4 nM inhibition, and RA283 demonstrating 5 nM of LRRK2-kinase inhibition in different LRRK2 kinase assays.

Selectivity profiling of over 300 protein kinases with each of these molecules reveals high selectivity. Off-target inhibition with IC_{50}< 500 nM identifies two other kinases (MST-2, MAP3K5) for PFE-360, three other kinases for MLi2 (MAP3K14, CLK4, CLK2), and two other kinases for RA283 (MLK1, ACK1), with selectivity for LRRK2 >10-fold compared with any other kinase.

Non-human primate (NHP) treatment

For the PFE-360 and MLi2-treated groups, female cynomolgus macaques, with an average age of 10 years (Xishan, PRC) were orally administered 5 mg kg^{-1} PFE-360 or MLi2 daily for five days (N = 5 per group, 10 total). Under anesthesia (Zoletil/atropine (6/0.04 mg/kg, IM), blood, urine (via acute catheterization), and CSF (from cisterna magna) were collected before treatment (baseline) and two hours post final treatment for a longitudinal assessment. Indices of LRRK2 inhibition were comparisons of baseline levels to those levels after drug-treatment.

For the RA283 treated groups, male cynomolgus macaques, ~3.5 years (Tamarinier and Noveprim), were orally administered RA283 at a low dose (10 mg kg^{-1}) and a high dose (30 mg kg^{-1}) regimen for seven days together with a vehicle-only group (n=2 per group, 6 total). All

procedures were performed in full compliance with standards for the care and use of laboratory animals, according to French and European Community (Directive 2010/63/EU) legislation, and approved by the local Animal Ethics Committee and the French Ministry for Research, under authorization H94-002-4 arrêté 2015-160 (10 December 2015). Urine, blood and CSF samples were collected 2 and 6 hours post final treatment for the low dose and high dose RA283 groups respectively. Indices of LRRK2 inhibition were comparisons of levels in the vehicle-only group to those in the low- and high-dose groups.

Drug plasma measurements

Unbound drug plasma concentrations were quantified by LC/MS analysis as previously described [23].

Exosome isolation

Urine (~200 µL to 1 mL) and CSF samples (~200 µL to 1 mL) were stored at -80°C in cryo-vials (Corning) and quick thawed in a water bath at 42°C before processing. Fluids were centrifuged at 10,000 x g for 30 minutes and the supernatants were transferred to polycarbonate centrifuge tubes. Samples were then centrifuged at 150,000 x g for 2 hours at 4°C. Supernatants were used for di-22:6-BMP analyses (below). Pellets (enriched in exosomes) were lysed in Laemmli buffer (4% SDS, 10% glycerol, 120 mM Tris pH 6.8, 40 mM NaF) freshly supplemented with 50 mg mL^{-1} DTT (dithiothreitol), and stored at -80°C.

Protein measurements

Peripheral blood mononuclear cells (PBMCs) were isolated from whole blood and lysed in Laemmli buffer (described above). Frontal cortices (300 mg) were lysed in Precellys tubes (CK14) in 1 ml RIPA buffer (1x, Cell Signaling) supplemented with phosphatase inhibitors (okadaic acid 1 µM and sodium fluoride 100 mM) and protease inhibitors (Complete cocktail, Sigma). After one-hour incubation at 4°C, lysates were centrifuged for 10 min at 4°C at 15,000 x g. Antibodies used include anti-LRRK2 (N241A/34, Antibodies Inc), anti-LRRK2 (clone MJFF2 c41-2, Abcam), anti-pS935 LRRK2 (clone UDD2-10, Abcam), anti-pS1292-LRRK2 (clone MJFR-19-7-8, Abcam), anti-pT73 Rab10 antibody (clone MJF-R21, Abcam), anti-Rab10 (clone D36C4, Cell Signaling), anti-flotillin-1 (clone D2V7J, Cell Signaling), and anti-TSG101 (ab30871, Abcam). The following secondary antibodies were used: HRP conjugated donkey

anti-rabbit secondary antibody (Jackson ImmunoResearch, # 711-035-152) and HRP conjugated donkey anti-mouse secondary antibody (Jackson ImmunoResearch, # 715-035-151). Immunoblots were developed using Luminata Crescendo Western HRP Substrate and digital signals were imaged and analyzed using ChemiDoc Imaging system (Bio-Rad) and ImageLab software (BioRad). Additionally, a homogeneous time-resolved fluorescence (HTRF) immunoassay was used for LRRK2 and pS935-LRRK2 according to manufacturer's guidelines (Cisbio). Recombinant full-length human G2019S-LRRK2 protein (Invitrogen) was used as a protein standard. Assay linearity and variably associated with each measure in the different biofluids was previously reported [13, 23, 67]. Standard curves with recombinant protein demonstrated linearity between 10 pg to 500 pg for total LRRK2 and 2.8pg to 140pg for pS1292-LRRK2 to (r>0.9) as shown previously [13]. Recombinant phospho-Rab proteins were not available for this study. Repeated measure analysis of four biofluid samples from NHPs limited to ~200 μL of starting biofluid volume showed a coefficient of variation (CV) better than 20%.

Di-docosahexaenoyl (22:6) bis (monoacylglycerol) phosphate measurement

Di-docosahexaenoyl (22:6) bis (monoacylglycerol) phosphate (di-22:6-BMP) was measured in plasma and exosome-depleted urine and CSF by ultra-performance liquid chromatography – tandem mass spectrometry (UPLC-MS/MS). The analyses were performed as previously described [25]. Standard curves were prepared using an authentic di-22:6-BMP reference standard. Di-22:6-BMP-d5 was used as an internal standard. Analyses were conducted using a Nextcea XR UPLC system (Shimadzu). A SCIEX X500B QTOF mass spectrometer with SCIEX OS software was used for quantitation (SCIEX). The calibration curve for di-22:6-BMP was linear between 0.05-100 ng mL^{-1} with ≥75% of the standards within ±15% (±20% for the lower-limit of quantitation) of the spiked concentration. Results at four quality-control concentrations (lower-limit, low, median, and high) showed that the assay was reproducible within ±15% of the nominal value (±20.0% at the lower-limit of quantitation). The concentrations of di-22:6-BMP measured in exosome-depleted urine were normalized to urine creatinine and reported as ng per mg of creatinine. Di-22:6-BMP values in exosome-depleted CSF were normalized by total protein and reported as ng per mg total protein.

Statistical Analysis

Two-tailed, paired t-tests were used to compare baseline and LRRK2 inhibitor treated samples. The median baseline was calculated for each marker and set to 1.0. Statistical analyses were performed using GraphPad Prism 5.0. When total protein was significantly impacted by treatment (i.e., treatment-induced reduction of total LRRK2 protein), the ratio of phospho to total-protein was considered critically confounded and interpreted with caution.

Data Availability

The datasets generated and/or analyzed during the current study are available from the corresponding author on reasonable request.

Acknowledgements

Research support was provided by NIH/NINDS U01 NS097028, R01 NS064934, and experiments were supported in-part by internal research programs at Atuka Inc, Sanofi, and Nextcea Inc. The corresponding author has full access to all the data and assumes final responsibility for the decision to submit for publication.

The authors thank Philippe Dugay, Stéphanie Eyquem and Isabel A. Lefevre (Sanofi, Rare and Neurologic Diseases Research), Manuela Pereira and Madeleine Coimbra (Sanofi, DMPK).

Author Contributions

All authors participated in study design, data analysis, drafting, and correction of this manuscript.

Competing Interests

S.W., K.K., and A.B.W. declare no competing conflicts of interest. L.D., S.B., and N.S. are employees of Sanofi and have shares in Sanofi. J.B.K. and J.M.B. are employees of Atuka and have shares in Atuka Inc. F.H. and E.T. are employed by Nexctea which holds patent rights to the di-22:6-BMP biomarker for neurological diseases involving lysosomal dysfunction (US 8,313,949, Japan 5,702,363, and Europe EP2419742).

Additional Information

Supplementary information is available for this paper.

Extended Data figures accompany the paper.

Correspondence and requests for materials should be addressed to A.B.W.

Reprints and permissions information is available at www.nature.com/reprints

Reporting Summary

Supplementary Figure Legends

Supplemental Figure 1. Structurally distinct small-molecule LRRK2 kinase inhibitors. a. The structure of PFE-360 is described as a morpholin-pyrrolopyrimidine (MW of 308 Da). The compound was synthesized at >98.4% purity **b.** The structure of MLi2 is described as an indazol-pyrimidine-morpholine (MW of 379 Da). The compound was synthesized at >97.4% purity. These compounds are structurally distinct pharmacophores.

Supplemental Figure 2. LRRK2 inhibition markers in PBMCs. Representative Western blots for LRRK2 and Rab10 before (-) and after (+) **a.** PFE-360 treatment or **b.** MLi2 treatment. PBMCs were isolated two hours after the final dose. 100pg and 10pg of recombinant LRRK2 were loaded as positive controls. Baseline pT73-Rab10 levels for NHP-1 fall below the limit of detection. All proteins were normalized to β-actin. NHP-1 demonstrated low baseline levels of pT73-Rab10 and was excluded from pT73-Rab10 biomarker measures for being below the limit of detection.

Supplemental figure 3. LRRK2 inhibition markers in urine. Urine was collected two hours after the final dose and exosomes were isolated by ultracentrifugation. Representative blots of LRRK2 and Rab10 before (-) and after (+) **a.** PFE-360 or **b.** MLi2 treatment. Exosomal proteins isolated from urine were normalized to the exosome marker TSG101. 100pg and 10pg of recombinant LRRK2 were loaded as positive controls.

Supplemental figure 4. LRRK2 inhibition markers in CSF. CSF was collected two hours after the final dose and exosomes were isolated by ultracentrifugation. Representative Western blots for LRRK2 in CSF exosomes before (-) and after (+) **a.** PFE-360 or **c.** MLi2 treatment. Exosomal proteins from CSF were normalized to the exosome marker flotillin-1. 100pg and 10pg of recombinant LRRK2 were loaded as positive controls. Di-22:6-BMP levels (ng mg^{-1} total protein) in exosome-depleted CSF before (baseline) and after **b.** PFE-360 or **d.** MLi2 treatment.

Supplemental Figure 5. LRRK2 inhibition in CSF exosomes of RA283 treated NHPs. a. Representative Western blots of LRRK2 inhibition in CSF exosomes after treatment with RA283at low dose (10 $mgkg^{-1}$), high dose (30 mg kg-^{1}) or vehicle control (M5-M6) for seven days. CSF samples were collected 2 and 6 hours after the final dose for low dose NHPs and high

dose NHPs, respectively. Exosomal proteins from CSF were normalized to the exosome marker flotillin-1.

Supplemental Figure 6. LRRK2 inhibition group measures for RA283. NHPs were treated with low dose (10 mg kg^{-1}), high dose (30 mg kg^{-1}), or vehicle control for seven days. Biofluids and tissue were collected 2 and 6 hours after the final dose for low dose NHPs and high dose NHPs, respectively. **a.** Effect of RA283 on Total LRRK2 levels in PBMC, urinary exosomes, CSF exosomes, and brain (frontal cortex). **b.** Effect of RA283 on pS935-LRRK2 levels in PBMC, urinary exosomes, and brain (frontal cortex). For CSF exosomes, pS1292-LRRK2 levels are indicated. **c.** Individual values are plotted with bars showing the group mean. One value is missing from the urinary exosome analysis (no sample for one low dose-treated animal).

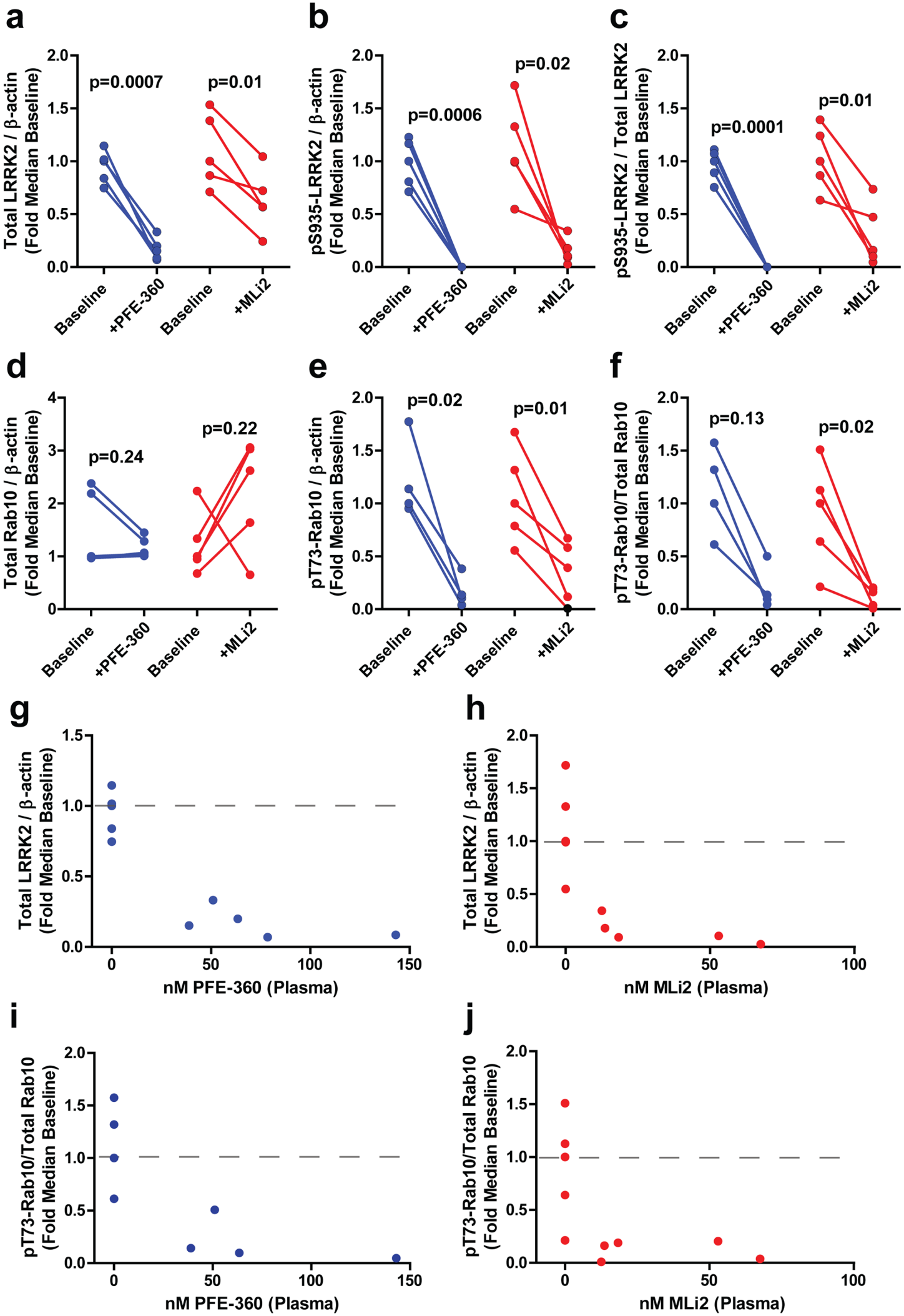
a
Total LRRK2 / β-actin (Fold Median Baseline)
p=0.0007
p=0.01
Baseline
+PFE-360
Baseline
+MLi2
b
pS935-LRRK2 / β-actin (Fold Median Baseline)
p=0.0006
p=0.02
c
pS935-LRRK2 / Total LRRK2 (Fold Median Baseline)
p=0.0001
p=0.01
d
Total Rab10 / β-actin (Fold Median Baseline)
p=0.24
p=0.22
e
pT73-Rab10 / β-actin (Fold Median Baseline)
p=0.02
p=0.01
f
pT73-Rab10/Total Rab10 (Fold Median Baseline)
p=0.13
p=0.02
g
Total LRRK2 / β-actin (Fold Median Baseline)
nM PFE-360 (Plasma)
h
Total LRRK2 / β-actin (Fold Median Baseline)
nM MLi2 (Plasma)
i
pT73-Rab10/Total Rab10 (Fold Median Baseline)
nM PFE-360 (Plasma)
j
pT73-Rab10/Total Rab10 (Fold Median Baseline)
nM MLi2 (Plasma)

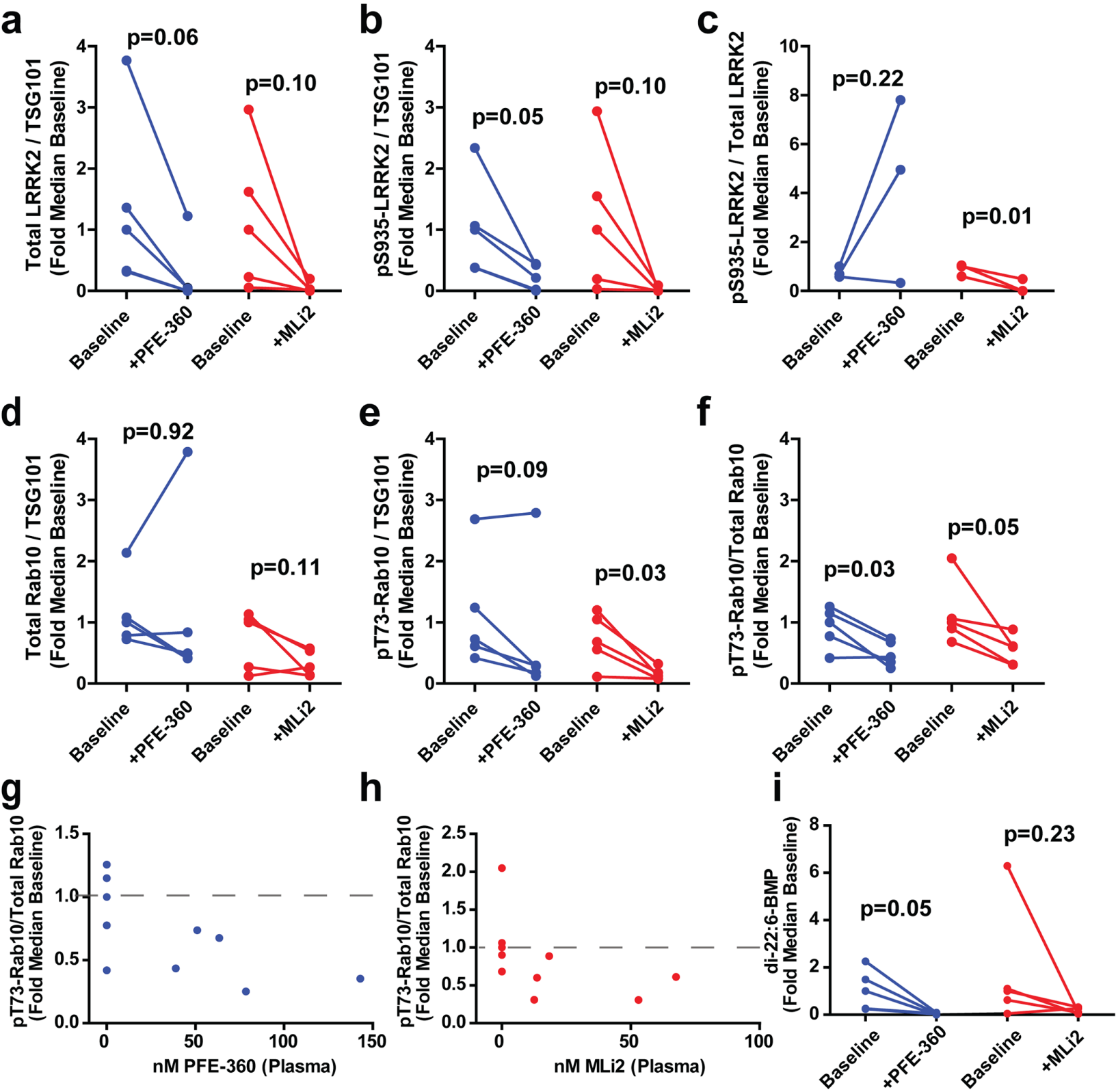
a
Total LRRK2 / TSG101 (Fold Median Baseline)
p=0.06
p=0.10
Baseline
+PFE-360
Baseline
+MLi2
b
pS935-LRRK2 / TSG101 (Fold Median Baseline)
p=0.05
p=0.10
c
pS935-LRRK2 / Total LRRK2 (Fold Median Baseline)
p=0.22
p=0.01
d
Total Rab10 / TSG101 (Fold Median Baseline)
p=0.92
p=0.11
e
pT73-Rab10 / TSG101 (Fold Median Baseline)
p=0.09
p=0.03
f
pT73-Rab10/Total Rab10 (Fold Median Baseline)
p=0.03
p=0.05
g
pT73-Rab10/Total Rab10 (Fold Median Baseline)
nM PFE-360 (Plasma)
h
pT73-Rab10/Total Rab10 (Fold Median Baseline)
nM MLi2 (Plasma)
i
di-22:6-BMP (Fold Median Baseline)
p=0.05
p=0.23

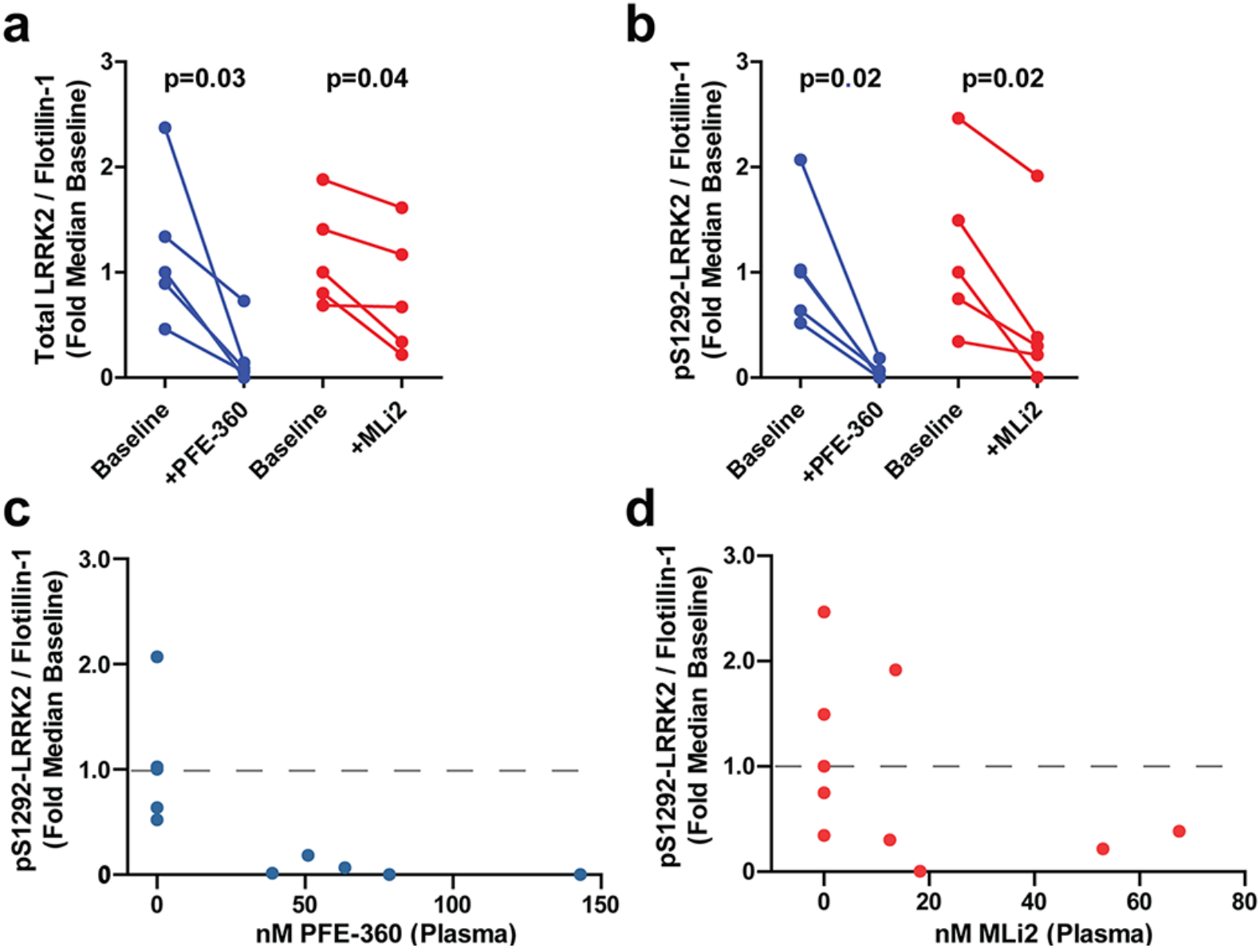
a
Total LRRK2 / Flotillin-1
(Fold Median Baseline)
p=0.03
p=0.04
Baseline
+PFE-360
Baseline
+MLi2
b
pS1292-LRRK2 / Flotillin-1
(Fold Median Baseline)
p=0.02
p=0.02
Baseline
+PFE-360
Baseline
+MLi2
c
pS1292-LRRK2 / Flotillin-1
(Fold Median Baseline)
nM PFE-360 (Plasma)
d
pS1292-LRRK2 / Flotillin-1
(Fold Median Baseline)
nM MLi2 (Plasma)

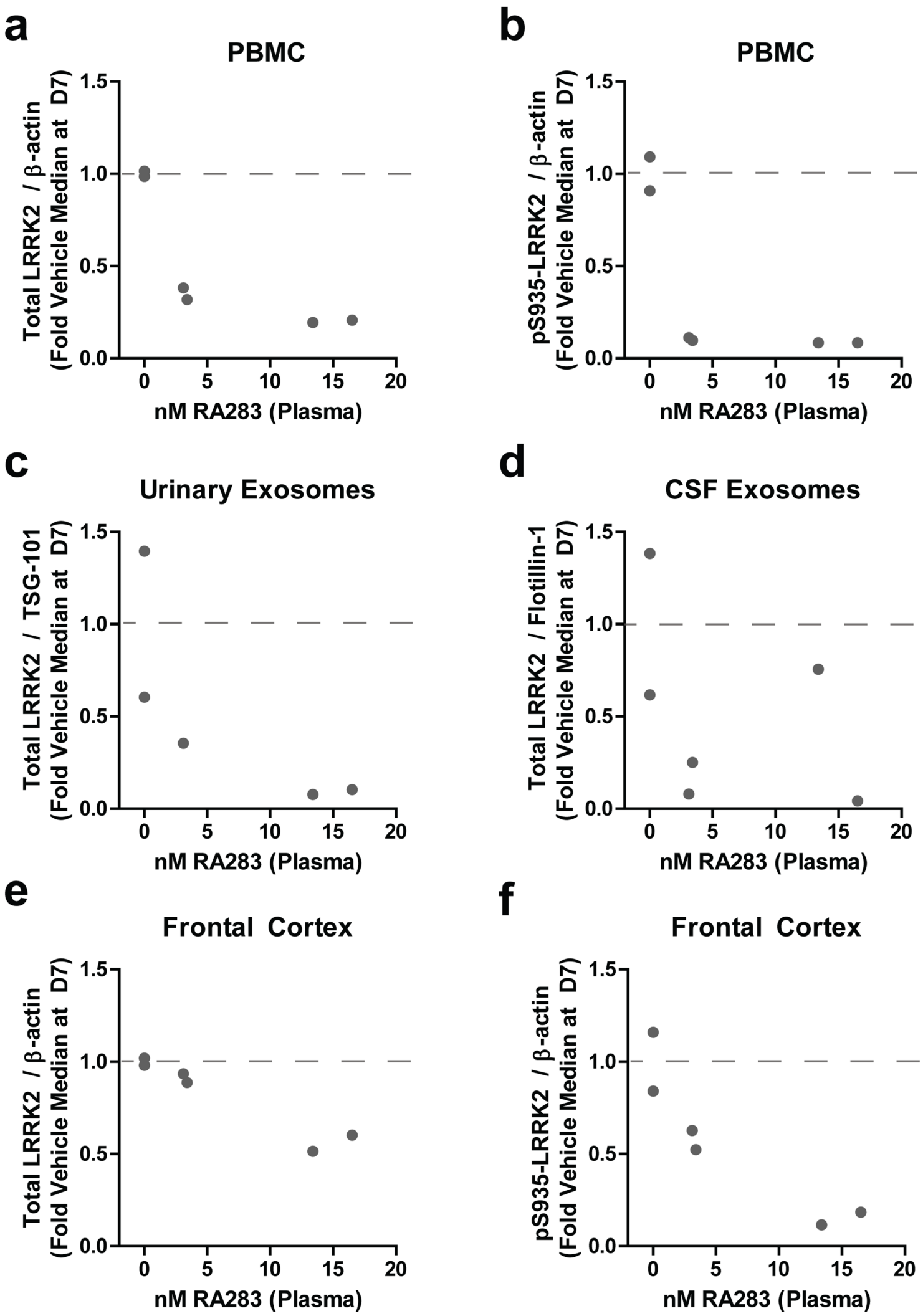
a
PBMC
Total LRRK2 / β-actin
(Fold Vehicle Median at D7)
1.5
1.0
0.5
0.0
0
5
10
15
20
nM RA283 (Plasma)
b
PBMC
pS935-LRRK2 / β-actin
(Fold Vehicle Median at D7)
1.5
1.0
0.5
0.0
0
5
10
15
20
nM RA283 (Plasma)
c
Urinary Exosomes
Total LRRK2 / TSG-101
(Fold Vehicle Median at D7)
1.5
1.0
0.5
0.0
0
5
10
15
20
nM RA283 (Plasma)
d
CSF Exosomes
Total LRRK2 / Flotillin-1
(Fold Vehicle Median at D7)
1.5
1.0
0.5
0.0
0
5
10
15
20
nM RA283 (Plasma)
e
Frontal Cortex
Total LRRK2 / β-actin
(Fold Vehicle Median at D7)
1.5
1.0
0.5
0.0
0
5
10
15
20
nM RA283 (Plasma)
f
Frontal Cortex
pS935-LRRK2 / β-actin
(Fold Vehicle Median at D7)
1.5
1.0
0.5
0.0
0
5
10
15
20
nM RA283 (Plasma)

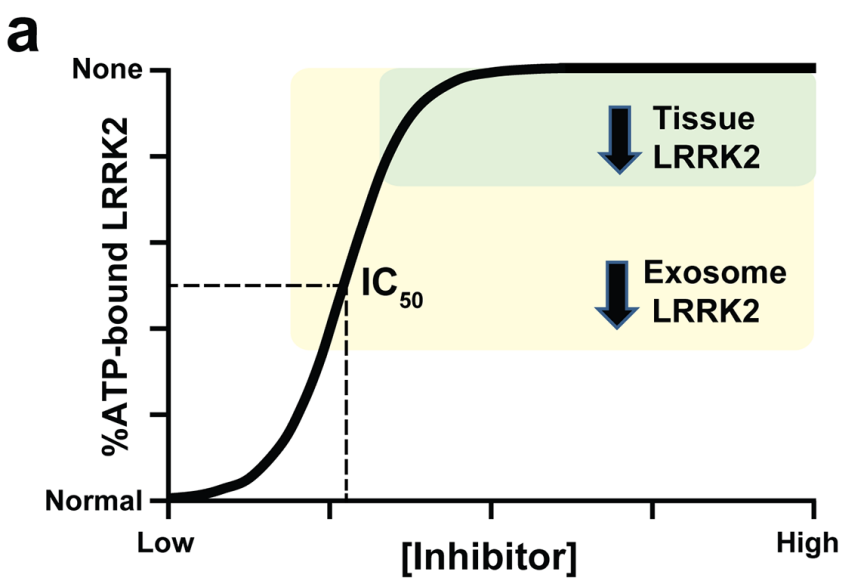
a
None
%ATP-bound LRRK2
Normal
Low
[Inhibitor]
High
IC50
Tissue
LRRK2
Exosome
LRRK2

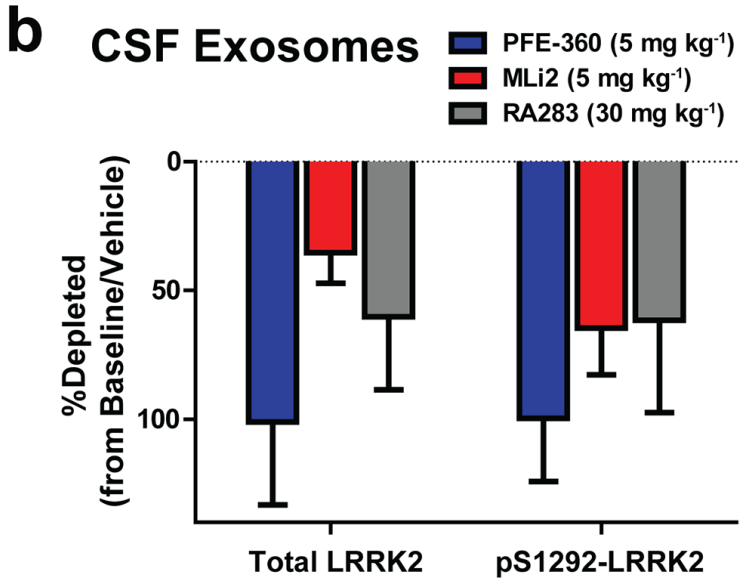
b
CSF Exosomes
PFE-360 (5 mg kg-1)
MLi2 (5 mg kg-1)
RA283 (30 mg kg-1)
%Depleted
(from Baseline/Vehicle)
0
50
100
Total LRRK2
pS1292-LRRK2